



9<sup>th</sup> Conference of the International Sports Engineering Association (ISEA)

## Investigations into soccer aerodynamics via trajectory analysis and dust experiments

John Eric Goff<sup>a\*</sup>, Matt J. Carré<sup>b</sup>

<sup>a</sup>*Lynchburg College, Department of Physics, Lynchburg, VA, 24501, USA*

<sup>b</sup>*University of Sheffield, Department of Mechanical Engineering, Sheffield, S1 3JD, UK*

Accepted 28 February 2012

---

### Abstract

We present a summary of our investigations into the aerodynamics of soccer balls (association footballs). Using a ball launcher and high-speed cameras, we are able to determine drag and lift coefficients using trajectory analysis. Advantages of this approach over wind tunnels include studying balls in flight without a support rod, which may influence aerodynamic studies in wind tunnels, and the ability to determine lift coefficients in regions inaccessible by many wind tunnels. We have found lift coefficients for spin parameters between 0 and 1 and Reynolds numbers between 130,000 and 300,000. Launching a ball into a dust cloud allows for the study of boundary-layer separation, again without the need of a support rod, which is needed for wind-tunnel studies. We have found boundary-layer separation angles in and around the drag crisis. Anomalous behavior is seen just past the drag crisis.

© 2012 Published by Elsevier Ltd.

*Keywords:* Soccer; football; drag; lift; spin parameter; boundary layer; trajectory analysis

---

### 1. Introduction

Aerodynamics of soccer balls (association footballs) in flight may be studied using a couple of different methods. Wind tunnels provide a way to subject balls to controllable air speeds. See, for example, work by Carré *et al* [1] and Asai *et al* [2] that examined soccer balls in wind tunnels. There are limitations to what wind tunnels can provide for aerodynamic studies. A support rod is needed to hold the ball in place. Expensive wind tunnels are usually needed if high air speeds are desired. There are also

---

\* John Eric Goff. Tel.: +1-434-544-8856; fax: +1-434-544-8646.

*E-mail address:* [goff@lynchburg.edu](mailto:goff@lynchburg.edu).

mechanical limitations on how fast a support rod can be turned if investigations into rotating balls are of interest.

Trajectory analysis provides an alternate way of examining the aerodynamics of soccer balls moving through air. The strategy is to film a projected soccer ball, analyze the resulting video so as to determine the time-dependent coordinates of the ball in a given plane, and then fit a computational solution of the equation of motion to those coordinates in order to determine aerodynamic coefficients. If just a single camera is used for filming, one must ensure that the ball's trajectory lies solely in one plane. Spinning balls may be studied if the spin axis is perpendicular to the plane of filming. Given the two aforementioned constraints, trajectory analysis may be used to study balls projected at various speeds and spin rates.

The remainder of this paper summarizes our trajectory analysis work. We have investigated [3-4] the aerodynamic properties of 32-panel and Teamgeist balls. We have also employed dust methods [5] to study boundary-layer separation on 32-panel balls.

## 2. Trajectory Physics

We are able to control the launch speed and initial spin rate of our projected soccer balls. The Reynolds number,  $Re$ , and spin parameter,  $Sp$ , both dimensionless, provide useful characterizations of a ball in flight. With the center-of-mass speed of the ball with respect to the still air far from the ball  $v$ , the ball's diameter  $D$ , and the kinematic viscosity  $\nu$ , the Reynolds number is defined as  $Re = vD/\nu$ . For the soccer balls we used,  $D \approx 0.218$  m and  $\nu \approx 1.54 \times 10^{-5}$  m<sup>2</sup>/s. Given that the game of soccer is played with speeds roughly in the range  $10 \text{ mph} \lesssim v \lesssim 70 \text{ mph}$  ( $4.5 \text{ m/s} \lesssim v \lesssim 31 \text{ m/s}$ ), the range of Reynolds numbers pertinent to soccer is approximately  $63,000 \lesssim Re \lesssim 440,000$ . A useful conversion between Reynolds number and soccer-ball speed is  $Re \times 10^{-5} \approx v/(7 \text{ m/s}) \approx v/(16 \text{ mph})$ .

The spin parameter is the ratio of a ball's equatorial tangential speed to its center-of-mass speed. With a ball radius  $r$  and angular speed  $\omega$ , the spin parameter is  $Sp = r\omega/v$ . Wind tunnels in some investigations [1-2] are capable of rotating balls such that  $Sp \lesssim 0.3$ . Our trajectory analysis approach allows us to reach  $Sp \approx 1$ .

While in the air, a soccer ball experiences two forces, one from the Earth and one from the air. The former force has magnitude  $mg$ , where  $m \approx 0.424$  kg is the ball's mass and  $g \approx 9.8 \text{ m/s}^2$  is the magnitude of the acceleration due to gravity near Earth's surface. The ball's weight is thus about 4.2 N. Though there is just a single force from the air, convention dictates splitting the air's force on the ball into various components. We neglect the buoyant force on the ball because it is less than 2% of the ball's weight. The component of the air's force opposite the direction of the ball's velocity is the drag force, which has magnitude given by  $F_D = \frac{1}{2} C_D \rho A v^2$ , where  $C_D$  is the dimensionless drag coefficient,  $\rho \approx 1.2 \text{ kg/m}^3$  is the air density, and the cross-sectional area of the ball is  $A \approx 0.0375 \text{ m}^2$ .

For balls spinning with angular velocity  $\vec{\omega}$ , the lift force usually points in the direction of  $\vec{\omega} \times \vec{v}$  and has magnitude  $F_L = \frac{1}{2} C_L \rho A v^2$ , where  $C_L$  is the dimensionless lift coefficient. There are circumstances under which the lift force points opposite the direction of  $\vec{\omega} \times \vec{v}$ , but those circumstances do not arise in our work here. The lift force is often called the Magnus force, though we are not concerned here with Magnus forces on non-spinning balls associated with surface irregularities. The lift force of interest for us is due solely from an asymmetric separation of the boundary layer of air because the ball is spinning. In all of our experiments with spinning soccer balls, we examined either pure backspin or pure topspin, meaning that all forces on the ball (weight, drag, and lift) lie in a plane.

Newton's second law provides the equation of motion for a soccer ball in flight. We refer the reader to our earlier work [3] for the mathematical treatment of this problem in two and three dimensions. In that work, we used Cartesian coordinates and showed how the drag and lift coefficients may, in principle, be



Fig. 1. (a) Our ball launcher projects a soccer ball; (b) Schematic of our experimental setup

extracted from trajectory data. Equations for the aerodynamic coefficients in such a treatment involve components of the ball's acceleration, which are notoriously unreliable when evaluated numerically from trajectory data. What we do instead is allow the aerodynamic coefficients to be free parameters in a numerical solution of the equation of motion. Those coefficients are varied until we minimize the square difference of the numerical solution with the trajectory data. Our trajectory analysis technique [3-4] thus allows for the determination of aerodynamic coefficients without the need for a support rod, as required in a wind tunnel, and for whatever initial speed and initial spin we can impart to the ball.

### 3. Experimental Procedure

We conducted our experiments in a sports hall at the University of Sheffield. An in-house designed ball launcher projected a soccer ball. Fig 1 shows our ball launcher and a schematic of the experimental setup. Four counter-rotating wheels on the ball launcher allow us to vary launch speed and initial spin rate. We kept initial speeds under 20 m/s and initial spin rates under 1700 rpm. We employed two high-speed cameras, one filming the launch and one filming the trajectory near the apex. The former camera records about 0.1 s of the initial motion; the latter films nearly 0.5 s of the middle of the trajectory. By syncing the two cameras' videos, we can fit a computationally-determined trajectory to the two sets of data. Typical still images from each camera are shown in Fig 2 (ball moves from right to left in figure).

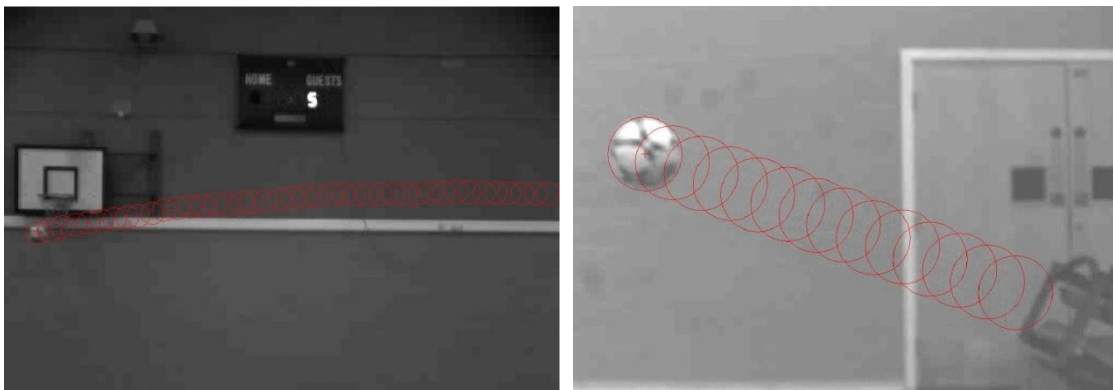


Fig. 2. (a) Trajectory points selected each 0.01 s from Camera 2; (b) Trajectory points selected each 0.005 s from Camera 1

If we launch at a speed that ensures that the ball’s speed never falls below the drag crisis ( $v \geq 14$  m/s), we may take  $C_D$  to be constant. If the ball does not spin, we may use the range of the ball, the initial launch velocity, the assumption of a constant  $C_D$ , and a computational solution of the equation of motion to determine the value of  $C_D$  that minimizes the square deviation between the trajectory data and the computational solution.

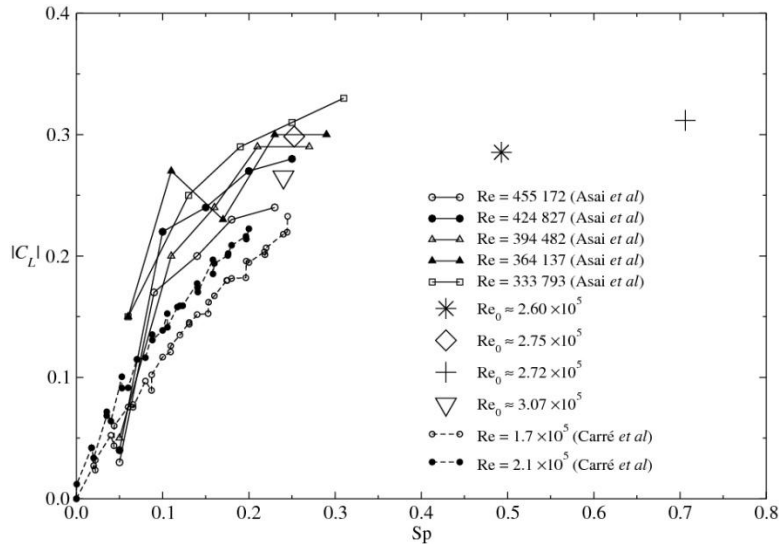


Fig. 3. (a)  $C_L$  vs.  $Sp$  for a 32-panel ball. Wind-tunnel data [1-2] also shown

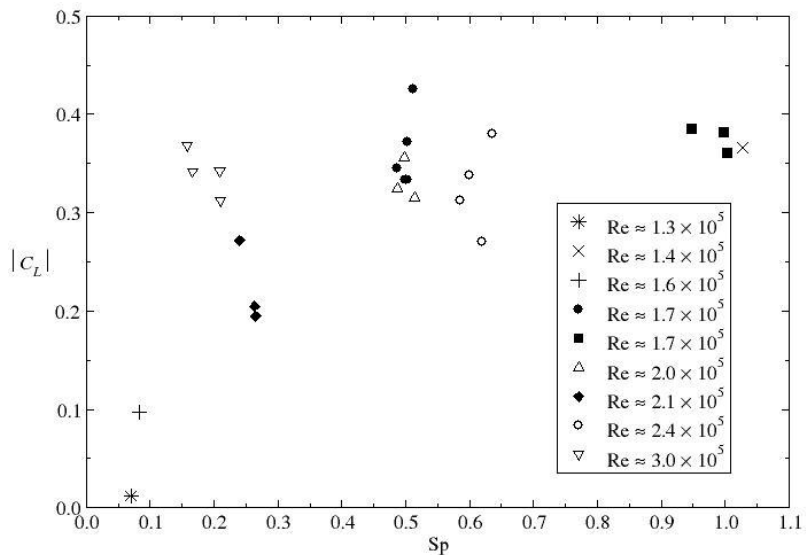


Fig. 3. (b)  $C_L$  vs.  $Sp$  for a Teamgeist ball

To get  $C_L$ , we use wind-tunnel data [2] for  $C_D$  as a function of spin rate and the data from Camera 1 only. By examining the ball’s trajectory near the launch, we ensure that the ball’s speed and spin rate do not change appreciably. We can then state a value of  $C_L$  for specific  $Re$  and  $Sp$  values.

#### 4. Aerodynamic Coefficients Results

When we analyzed the flight of a non-spinning ball such that  $2.23 < \text{Re} \times 10^{-5} < 2.76$  ( $15.6 \text{ m/s} < v < 19.3 \text{ m/s}$ ) over the entire trajectory, we found that  $C_D \approx 0.17$ , which is consistent with wind-tunnel data [2]. Our primary interest was in finding  $C_L$  for  $\text{Sp}$  values inaccessible in many wind tunnels. We began with a modest number of trials using a 32-panel ball, and then proceeded to use a Teamgeist ball for many trials. Fig 3 shows our results for  $C_L$  as a function of  $\text{Sp}$ . Fig 3a for a 32-panel ball shows that for  $\text{Sp} < 0.3$ , we matched wind-tunnel data. The data we show well beyond  $\text{Sp} = 0.3$  suggest a leveling off for  $C_L$ . That  $C_L$  levels off with  $\text{Sp}$  is further demonstrated in Fig 3b for a Teamgeist ball. To offer an idea of the numbers seen in Fig 3b, note that if  $v \approx 14 \text{ m/s}$ , which corresponds to  $\text{Re} \approx 2 \times 10^5$ , and  $\text{Sp} \approx 0.5$ , then the angular speed is  $\omega \approx 63.6 \text{ rad/s} \approx 608 \text{ rpm}$ . For the aforementioned values, Fig 3b shows that  $C_L \approx 0.35$ .

#### 5. Boundary-Layer Separation via Dust Experiments

Having used a ball launcher and trajectory analysis for the determination of aerodynamic coefficients, we moved on to a study [5] of the separation of the boundary layer from a soccer ball. Instead of using a wind tunnel for such an investigation, we used our ball launcher to fire a soccer ball into a cloud of dust made simply by clapping a handful of rock-climbing chalk dust over a region of space just before a ball passed through that region. A high-speed camera recorded the ball passing through the dust. By analyzing the video, we could ascertain the separation angle,  $\phi$ , of the boundary layer. The angle  $\phi$  is measured on the back of the ball between the intersection of the two lines joining the separation points and the center of the ball. Fig 4 shows two typical images of a ball passing through a dust cloud. Fig 4a shows a ball moving at a speed below the drag crisis; Fig 4b shows a ball moving at a speed above the drag crisis. We see in Fig 4 the expected result that the boundary layer separates farther back on the ball above the drag crisis compared to the separation below the drag crisis [6].

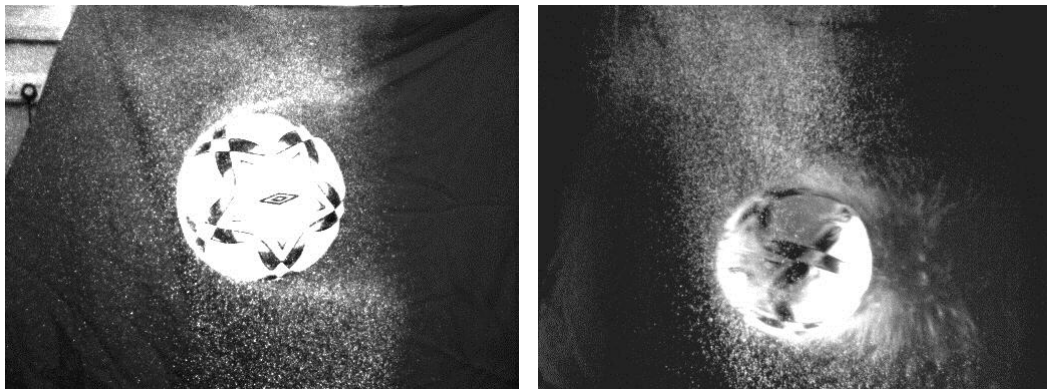


Fig. 4. (a) Below drag crisis:  $v \approx 7.65 \text{ m/s}$ ,  $\phi \approx 198^\circ$ ; (b) Above drag crisis:  $v \approx 19.14 \text{ m/s}$ ,  $\phi \approx 97^\circ$ . Note behind the ball the black cloth that allows one to better see the white dust

Our speed region of interest is in the drag crisis. We performed 16 tests using a 32-panel soccer ball in the speed range given by  $6.58 \text{ m/s} \lesssim v \lesssim 19.63 \text{ m/s}$  ( $94,000 \lesssim \text{Re} \lesssim 280,000$ ). For our initial investigations our tests consisted of non-spinning balls only. Figure 5 shows the main results of this study. Also shown is a fitted curve [5] to wind-tunnel data [2] for the drag coefficient of a non-spinning 32-panel ball. The precipitous drop in  $C_D$  is in the region known as the drag crisis. Tests 1-9 have a separation angle in the range  $177^\circ \lesssim \phi \lesssim 206^\circ$ . For all tests, we are able to examine a ball in the

configuration seen in still images like those in Fig 4. We can then ascertain whether or not the boundary layer separates at the top and bottom of the ball near a seam or near a smooth patch. For tests 1-9, we found smaller values of  $\phi$  when separation occurred near seams compared to separation near smooth patches. That is consistent with the notion that rough areas on a ball's surface delay the separation of the boundary-layer.

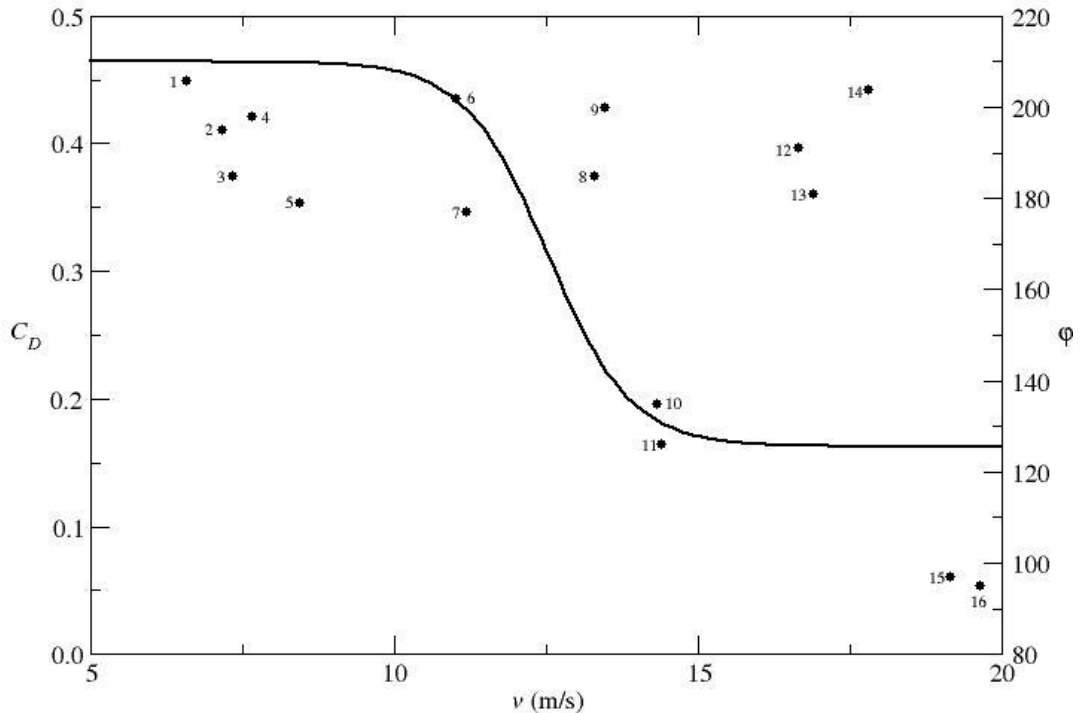


Fig. 5. Boundary-layer separation angle (in degrees),  $\phi$  (right vertical axis), vs. ball speed,  $v$ . The drag coefficient (left vertical axis) fitted from wind-tunnel data [2] is also shown

Increasing speed through the drag crisis, we see in tests 10 and 11 a drop in  $\phi$ . Tests 15 and 16 show a continued drop in  $\phi$  as the speed nears 20 m/s. We expected this because, as Fig 4 shows, our initial understanding is that  $\phi$  is smaller beyond the drag crisis compared to its values below the drag crisis. We did not expect the results of tests 12-14. For those tests, the separation angle is  $181^\circ \leq \phi \leq 204^\circ$ , a range that is more in line with tests 1-9. At present we do not understand this anomalous jump in the separation angle after the drag crisis. Understanding that jump will be the subject of a future investigation.

## References

- [1] Carré MJ, Goodwill SR, and Haake SJ. "Understanding the effect of seams on the aerodynamics of an association football." *J Mech Eng Sci* 2005; 219:657-66.
- [2] Asai T, Seo K, Kobayashi O, and Sakashita R. "Fundamental aerodynamics of the soccer ball." *Sports Eng* 2007; 10:101-10.
- [3] Goff JE and Carré MJ. "Trajectory analysis of a soccer ball." *Am J Phys* 2009; 77: 1020-7.
- [4] Goff JE and Carré MJ. "Soccer ball lift coefficients via trajectory analysis." *Euro J Phys* 2010; 31: 775-84.
- [5] Goff JE, Smith WH, and Carré MJ. "Football boundary-layer separation via dust experiments." *Sports Eng* 2011; 14: 139-46.
- [6] Goff JE. "Power and spin in the beautiful game." *Physics Today* 2010; 63: 62-3.